International Journal of Applied Science and Engineering
2013. 11, 3: 251-266

Bi-Performance Optimization of End Milling Characteristics of Al/SiCp Composites Using NSGA-II

R. Arokiadass*, K. Palaniradja, and N. Alagumoorthi

Department of Mechanical Engineering, Pondicherry Engineering College, Puducherry, India

Abstract: Optimization of process parameters is important to achieving high quality in the machining process, especially where more complex multiple performance optimization is required. The present investigation focuses on the multiple performance optimization on end milling characteristics of LM25 Al/SiCp metal matrix composites. The process parameters used for the experiments were spindle speed, feed rate, depth of cut, and percentage weight of silicon carbide. Experiments were carried out according to response surface methodology (RSM). Statistical models were developed for tool flank wear and surface roughness. These models were used for optimization by which the optimum parameter settings were obtained with a view to minimizing the responses. The Non-dominated Sorting Genetic Algorithm (NSGA-II) tool was used to optimize the cutting conditions, yielding a non-dominated solution set that is reported here.

Keywords: Metal matrix composites; end milling; modeling; optimization; non-dominated sorting genetic algorithm (NSGA-II).

1. Introduction

New research in the material science has been directed towards the development of new light weight engineering materials processing high specific strength and stiffness at elevated temperatures and good creep, fatigue and wear resistance. That is because advanced automotive and aerospace technology requires these materials to improve performance. Particulate reinforced MMCs have received considerable attention due to their low cost when compared to long fiber reinforced MMCs and due to their better properties than those of monolithic alloys [1]. These materials may have a wide application, especially for components, which are exposed to friction [2]. The most popular reinforcements are silicon carbide and alumina. Aluminium, titanium and magnesium alloys are commonly used as the matrix phase. It is possible to produce high quality MMC components to near-net shape through various manufacturing techniques, but component design and dimensional tolerance requirements, the need for machining cannot be completely eliminated.

End milling process is classified as material removal process. This process and its machine tools are capable of producing complex shapes with the use of multi tooth cutting tools. In the end milling process, a multi tooth cutter rotates along various axes with respect to the workpiece. Wear on the flank of a cutting tool is caused by friction between the newly machined workpiece surface and the contact area on the tool flank. Because of the rigidity of the workpiece, the worn

* Corresponding author; e-mail: raja_arokiadass@yahoo.com

Received 8 June 2012
Revised 7 December 2012
Accepted 22 February 2013

area referred to the flank wear land, must be parallel to the resultant cutting direction. The width of the wear land is usually taken as a measure of the amount of wear and can be readily determined by means of a toolmaker's microscope. In the end, excessive flank wear will lead to poor surface texture, inaccuracy and increasing friction as the edge shape changes.

Several studies have been done in order to examine the efficiency of different cutting tool materials, such as cemented carbide, coated carbide, and diamond in turning, milling, drilling, reaming, and threading of MMC materials. The main problem while machining MMC is the extensive tool flank wear caused by the very hard and abrasive reinforcements. Manna et al. [1] investigated the machinability of Al/SiC MMC and found that no built-up edge (BUE) is formed during machining of Al/SiC MMC at high speed and low depth of cut and also observed a better surface finish at high speed with low feed rate and low depth of cut.

Suresh Kumar Reddy et al. [3] studied quality of components produced during end milling of Al/SiC particulate metal matrix composites (PMMCs). The results showed that the presence of the reinforcement enhances the machinability in terms of both surface roughness and lower tendency to clog the cutting tool, when compared to a non-reinforced Al alloy. These results would serve to understand that the end milling machining process can provide better inputs to ensure better machining of Al/SiC PMMC and are expected to lead technological and economical gains with the use of Al/SiC PMMC in various industrial applications by replacing Al alloys. Li and Seah [4] studied the effect of size and volume content of SiC particles in machinability of MMC. According to their results, when the amount of reinforcement is more than some critical percentage, the tool wear is more severe.

Ozben et al. [5] investigated the mechanical properties and the effects of machining parameters on tool wear and surface roughness of silicon carbide particulate (SiCp) reinforced aluminum MMC for different volume fraction. It was observed that the increase in reinforcement addition produced better mechanical properties such as impact toughness and hardness. The machinability properties of the selected material were studied and higher SiCp reinforcement produced a higher tool wear. The surface roughness was generally affected by feed rate and cutting speed. Mathematical modeling in terms of process parameters for tool wear has been carried out by many researchers. Kaye et al. [6] developed a mathematical model based on response surface methodology to predict tool flank wear using spindle speed change.

However, for the practical machining of Al/SiCp metal matrix composite, optimal machining parameters must be determined to achieve less tool wear and surface roughness. This paper discusses the application of the Non-dominated Sorting Genetic Algorithm (NSGA-II) to optimize the machining parameters for machining Al/SiCp composites with multiple characteristics. The principles of multiple performance optimization differ from those of single performance optimization. In multi-performance optimization, there is more than one objective function, each of which may have a different optimal solution. Most of the time these objectives conflict with one another (i.e., optimizing one objective compromises the other objectives) [7, 8].

The Genetic Algorithm (GA) is an evolutionary algorithm. It is based on the mechanics of natural selection and it combines the characteristics of direct search and probabilistic selection methods. It is a very simple yet powerful tool for obtaining global optimum values for multi-model and combinatorial problems. The GA works with a population of feasible solutions and, therefore, it can be used in multi-objective optimization problems to simultaneously capture a number of solutions [9]. In a typical multi-objective optimization problem, there exists a set of solutions which are superior to the other solutions in the search space, when all objectives are considered, but which are inferior to other solutions in the space with respect to one or more objectives. These are known as Pareto-optimal solutions or non-dominated solutions. The rest of the solutions are known as dominated solutions [7]. GA based multi-objective optimization methodologies have adequately demonstrated their usefulness in finding a well-converged and well-distributed set of near Pareto-optimal solutions [7, 10]. The Non-dominating Sorting GA-II (NSGA-II) is a fast, elitist multi-objective genetic algorithm that is widely used for generating the Pareto frontier. Its main advantage in solving multi-objective problems is that it leads the search toward the global Pareto front while maintaining diversity of the solution set along that front [11].

This study focuses on the end milling characteristics of Al/SiCp composites, whose field of application is constantly growing. The machining tests were performed on a vertical milling machine using an uncoated solid end mill cutter. The experiments were designed using response surface methodology. The process parameters-spindle speed, feed rate, depth of cut and various percentage weight of silicon carbide were optimized with multiple response characteristics including tool flank wear and surface roughness. Models were developed for tool flank wear and surface roughness. These models were used for optimization by which the optimum parameter settings were obtained with a view to minimizing tool flank wear and minimizing surface roughness. The NSGA-II algorithm was used to optimize the Al/SiCp composite machining process. The method presented here may be useful in a machine and/or manufacturing shop.

2. Experimental work

The work material used for the present investigation is LM 25Al/SiCp metal matrix composites with dimensions of 100 mm × 50 mm × 40 mm. The composites were manufactured by a stir casting method. The experiments were planned using CCD for the design of experiments (DOE), which helps reduce the number of experiments. Four machining parameters were selected: spindle speed, feed rate, depth of cut and percentage weight of silicon carbide. Since the considered factors are multi-level variables whose outcome effects are not linearly related, it was decided to use five level tests for each factor. The machining parameters used and their levels are presented in Table 1.

The end milling experiments have been conducted in CNC HASS vertical milling machine using uncoated solid carbide cutters, having diameter of 12 mm, helix angle of 45º, rake angle of 10º and number of flutes 4. Experiments have been conducted according to central composite second order rotatable design (CCD) as depicted in Table 2. In the present study, the machining performance was evaluated by the following responses:

Table 1. Experimental parameters and their levels

Process parameters	Unit	Notation	Levels				
			(-2)	(-1)	0	(+1)	(+2)
Spindle speed	RPM	N	2000	2500	3000	3500	4000
Feed rate	mm/rev	f	0.02	0.03	0.04	0.05	0.06
Depth of cut	mm	d	0.5	1	1.5	2	2.5
Silicon Carbide	%wt	S	5	10	15	20	25

Table 2. Experimental results

Ex.No	N (RPM)	f ((mm/rev)	d (mm)	S (%wt.)	VB_{max}, mm	R_a, μm
1	2500	0.03	1	10	0.224	4.406
2	3500	0.03	1	10	0.284	3.812
3	2500	0.05	1	10	0.258	6.034
4	3500	0.05	1	10	0.291	5.229
5	2500	0.03	2	10	0.235	4.472
6	3500	0.03	2	10	0.294	3.802
7	2500	0.05	2	10	0.270	6.032
8	3500	0.05	2	10	0.297	5.312
9	2500	0.03	1	20	0.338	4.978
10	3500	0.03	1	20	0.407	4.395
11	2500	0.05	1	20	0.377	6.789
12	3500	0.05	1	20	0.422	5.945
13	2500	0.03	2	20	0.358	5.071
14	3500	0.03	2	20	0.413	4.402
15	2500	0.05	2	20	0.384	6.804
16	3500	0.05	2	20	0.419	6.054
17	2000	0.04	1.5	15	0.262	6.202
18	4000	0.04	1.5	15	0.361	4.638
19	3000	0.02	1.5	15	0.314	3.679
20	3000	0.06	1.5	15	0.357	7.008
21	3000	0.04	0.5	15	0.309	5.062
22	3000	0.04	2.5	15	0.341	5.299
23	3000	0.04	1.5	5	0.211	4.334
24	3000	0.04	1.5	25	0.443	5.639
25	3000	0.04	1.5	15	0.322	5.183
26	3000	0.04	1.5	15	0.328	5.177
27	3000	0.04	1.5	15	0.319	5.221
28	3000	0.04	1.5	15	0.326	5.163
29	3000	0.04	1.5	15	0.323	5.155
30	3000	0.04	1.5	15	0.327	5.199
31	3000	0.04	1.5	15	0.329	5.229

2.1. Tool flank wear

Keeping tool wear to a minimum is another important criterion, since it will affect the part size and quality (e.g., surface finish) of products [12, 13]. There are four general wear zones on a typical cutting tool viz: crater wear, flank wear, nose radius wear and notch wear. Among these, flank wear is the most important and gives an overall indication of the wear process. Flank wear produces wear lands on the side and end flanks of the tool because of the rubbing action of the machined surface, which has been considered in this work and measured using a toolmaker's microscope. The experimental results are presented in Table 2.

2.2. Surface roughness

Surface finish is another important aspect in the machining of composites. The average surface roughness (Ra), which is mostly used in industry, is taken up for the present study. The surface roughness was measured a number of times and averaged. The surface roughness of test pieces has been measured using Talysurf tester with a sampling length of 10mm. The experimental results are presented in Table 2.

3. Statistical modeling

The Response surface modelling is a useful tool for searching out the relationship between various process parameters and the machining criteria of a machining process to explore the effect of these parameters on the response criteria of the machining process. The objective of the Response surface modelling is to develop the mathematical link between the response and predominant machining parameters. The general second order polynomial response surface mathematical model can be considered to evaluate the parametric influences on the various criteria as follows:

$$Y_u = b_0 + \sum_{i=1}^{k} b_i x_i + \sum_{i=1}^{k} b_{ii} x_i^2 + \sum_{j>1}^{k} b_{ij} x_i x_j \tag{1}$$

where Y_u is the corresponding response, b_i represents the linear effect of x_i, b_{ii} represents the quadratic effect of x_i and b_{ij} reveals the linear-by-linear interaction between x_i and x_j.

Owing to wide ranges of factors, it was decided to use four factors, five levels, and rotatable CCD matrix to optimize the experimental conditions. The main objective of the factorial experiments consists of studying the relationship between the response as a dependent variable and the parameter levels. This approach helps to understand in a better way, how the change in the levels of application of a group of parameters affects the response. A combination of the levels of the parameter, which leads to certain optimum response, can also be located through this approach. In order to investigate the influence of process parameters on the flank wear (VB_{max}) and surface roughness (Ra) four principal process parameters such as the spindle speed (N), feed rate (f), depth of cut (d), and percentage weight of silicon carbide (S) were taken. In this study, these process parameters were chosen as the independent input variables. The desired responses were the flank wear (VB_{max}) and the surface roughness (Ra) which are assumed to be affected by the above four principal process parameters. A 2^k factorial with central composite second order rotatable design was used (in this case k=4). This consists of $n_c=2^k=16$ corner points at +1 level, $n_a=2^k=8$ axial points at $\gamma=+2$, and a centre point at zero level repeated seven times n_0 to estimate the pure error.

Statistical models based on second-order polynomial equation (1) were developed for tool flank wear and surface roughness using the experimental results and are given below:

$$\begin{aligned}\text{Tool flank wear (VBmax)} = {} & -0.2551 + (0.0002\ X1) + (2.4923\ X2) + (0.0404\ X3) \\ & + (0.0084\ X4) + (34.4196\ X22) + (0.0033\ X32) \\ & + (0.0001\ X42) - (0.0013\ X1\ X2) - (0.3125\ X2\ X3) \\ & + (0.0088\ X2\ X4) - (0.0002\ X3\ X4)\end{aligned} \tag{2}$$

$$\begin{aligned}\text{Surface roughness (Ra)} = {} & 4.716 - (0.002\ X1) + (61.948\ X2) + (0.050\ X3) \\ & + (0.099\ X4) + (365.551\ X22) - (0.017X32) - (0.002\ X42) \\ & - (0.008\ X1\ X2) + (0.612\ X2\ X3) + (0.789\ X2\ X4) + (0.002\ X3\ X4)\end{aligned} \tag{3}$$

Here spindle speed (X_1) is in RPM, feed rate (X_2) is in mm/rev., depth of cut (X_3) is in mm and various percentage weight of silicon carbide (X_4).

4. NSGA-II algorithm

The Non-dominated Sorting Genetic Algorithm, which was introduced by Srinivas and Kalyanmoy [7], has been criticized for its high computational complexity, lack of elitism and its choice of the optimal parameter value for sharing parameter σ. The NSGA-II is a modified version, which has a better sorting algorithm, incorporates elitism and does not require the choosing of a sharing parameter a priori. The flow chart of the NSGA-II is shown in Figure 1.

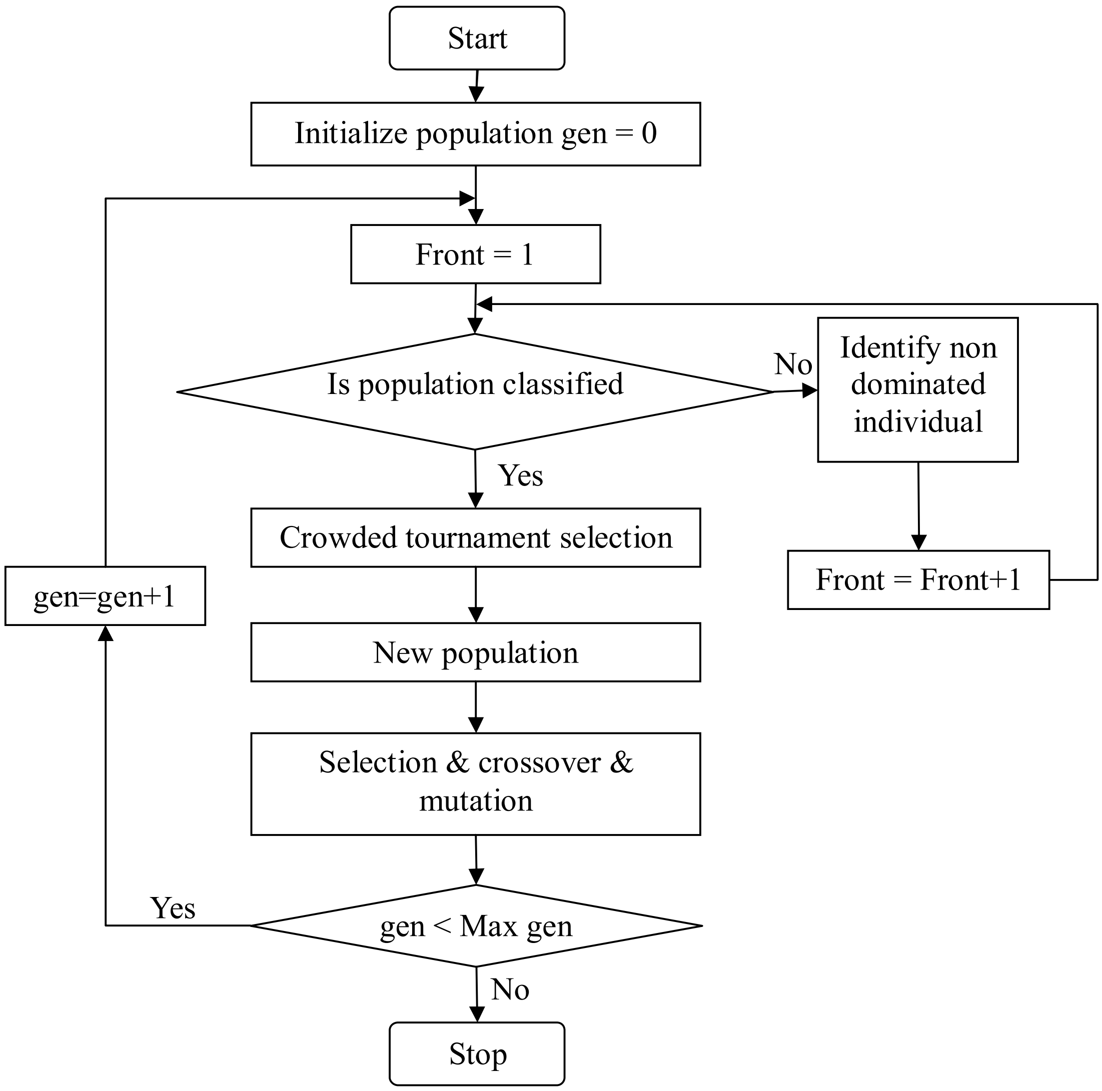

Figure 1. Flow chart of NSGA-II program

4.1. Description of NSGA-II algorithm

The steps involved in the solution of optimization problem using NSGA-II are as follows.

1. *Population Initialization*. The population is initialized based on the problem range and

constraints if any.

2. *Non-Dominated sort.* The initialized population is sorted based on non-domination. The fast sort algorithm is described as below.

For each individual p in main population P:

(a) Initialize $S_p = \phi$. This set would contain all the individuals that are being dominated by p.

(b) Initialize $n_p = 0$. This would be the number of individuals that dominate p.

For each individual q in P:

(a) If p dominates q then add q to the set S_p, i.e.,

$$S_p = S_P \cup \{q\} \tag{4}$$

(b) Else if q dominates p then increment the domination counter for p, i.e.,

$$n_p = n_p + 1 \tag{5}$$

(c) If $n_p = 0$, i.e., no individuals dominate p then p belongs to the first front. Set rank of individual p to 1, i.e., $P_{rank} = 1$. Update the first front set by adding p to front one, i.e.,

$$F_1 = F_1 \cup \{p\} \tag{6}$$

(d) This is carried out for all the individuals in main population P.

(e) Initialize the front counter to one, i = 1.

(f) The following is carried out while the i^{th} front is nonempty, i.e., $F_i \neq \phi$.

$Q = \phi$. The set for storing the individuals for $(i + 1)^{th}$ front.

For each individual p in front F_i

(a) For each individual q in S_p (S_p is the set of individuals dominated by p).

(b) If set $n_q = n_q - 1$, decrement the domination count for individual q.

(c) If $n_q = 0$ then none of the individuals in the subsequent fronts would dominate q. Hence set $q_{rank} = i + 1$. Update the set Q with individual q, i.e.,

$$Q = Q \cup \{q\} \tag{7}$$

(d) Increment the front counter by one.

(e) Now the set Q is the next front and hence $F_i = Q$.

This algorithm is better than the original NSGA [10] since it utilizes the information about the set that an individual dominate (*Sp)* and number of individuals that dominate the individual (n_p).

3. *Crowding Distance.* Once the non-dominated sort is complete the crowding distance is assigned. Since the individuals are selected based on rank and crowding distance all the individuals in the population are assigned a crowding distance value. Crowding distance is assigned front wise and comparing the crowding distance between two individuals in different front is meaningless [10]. The crowing distance is calculated as below.

For each front F_i, n is the number of individuals.

(a) Initialize the distance to be zero for all the individuals, i.e., $F_i(d_j) = 0$, where j corresponds to the j^{th} individual in front F_i.

(b) For each objective function m.

(c) Sort the individuals in front F_i based on objective m, i.e., I = sort (F_i, m).

(d) Assign infinite distance to boundary values for each individual in F_i, i.e.,

$$I(d_1) = \infty \quad \text{and} \quad I(d_n) = \infty \tag{8}$$

Where, $I(d_1)$ and $I(d_n)$ are the distances between the extreme solutions and the boundary solutions of the obtained nondominated set.

For $k = 2$ to $(n-1)$

$$.I(d_k) = I(d_k) + \frac{I(k+1).m - I(k-1).m}{f_m^{\max} - f_m^{\min}} \tag{9}$$

I (*k*)*.m* is the value of the m^{th} objective function of the k^{th} individual in *I*. $f_m^{\max}$ *and* $f_m^{\min}$ are the maximum and minimum value of the objective function f_m.

The basic idea behind the crowing distance is finding the Euclidian distance between each individual in a front based on their m objectives in the *m* dimensional hyper space. The individuals in the boundary are always selected since they have infinite distance assignment.

4. *Selection*

Once the individuals are sorted based on non-domination and with crowding distance assigned, the selection is carried out using a *crowded-comparison-operator* ($\prec_n$). The comparison is carried out as below based on

(a) non-domination rank p_{rank} i.e. individuals in front F_i will have their rank as $p_{rank} = i$.

(b) crowding distance $F_i(d_j)$

$p \prec_n q$ if

$$p_{rank} < q_{rank} \tag{10}$$

or if *p* and *q* belong to the same front *Fi* then $Fi(d_p) > Fi(d_q)$ i.e. the crowing distance should be more.

The individuals are selected by using a binary tournament selection with crowed-comparison-operator.

5. *Genetic Operators.* Real-coded GA's use Simulated Binary Crossover (SBX) operator for crossover and polynomial mutation [14].

(a) Simulated Binary Crossover.

The SBX operator works with two parent solutions and creates two offspring. The difference between offspring and parent depends on crossover index η_c. It has two properties: (a) the difference between corresponding decision variables of the created offspring is proportional to the difference between corresponding decision variables of the parent solutions; (b) offspring having decision variables nearer to those of the parent solutions are more likely to be selected. The procedure for finding the offspring solutions $x_j^{(1,t+1}$ and $x_i^{(2,t+1}$ from parent solutions $x_j^{(1,t)}$ and $x_i^{(2,t)}$ is given below: A spread factor β_i is defined as the ratio of the absolute difference in children values to that of the parents:

$$\beta_i = (x_j^{(1,t+1)} - x_i^{(2,t+1)}) / (x_j^{(1,t)} - x_i^{(2,t)}) \tag{11}$$

First a random number u_i between 0 and 1 is created. Thereafter, from a specified probability distribution function, the ordinate β_{qi} is found so that the area under the probability curve from 0 to β_{qi} is equal to the chosen random number u_i :

Application of A Fast and Elitist Multi-Objective Genetic Algorithm to Reactive...

$$P(\beta_i) \begin{cases} 0.5(\eta_c + 1)\, \beta_i^{\eta c}, & \text{if } \beta_i \le 1; \\ 0.5(\eta_c + 1)\, \dfrac{1}{\beta i^{\eta_c + 2}}, & \text{otherwise} \end{cases} \tag{12}$$

This distribution can be obtained from a uniformly sampled random number u_i between (0,1). η_c is the distribution index for crossover.

Using equation 13, calculate β_{qi} by equating the area under the probability curve equal to u_i as follows:

$$\beta_{qi} = \begin{cases} (2u_i)^{\frac{1}{(\eta_c+1)}}, & \text{if ui} \leq 0.5; \\ \left(\frac{1}{2(1-u_i)}\right)^{\frac{1}{(\eta_c+1)}}, & \text{otherwise.} \end{cases} \tag{13}$$

In the above equations (11, 12), the distribution index η_c is any positive real number. After obtaining β_{qi}, the children solutions are calculated as follows:

$$x_j^{(1,t+1)} = 0.5\,[\,(1+\beta_{qi})\,x_j^{(1,t)} + (1-\beta_{qi})\,x_j^{(2,t)}\,],$$

$$x_i^{(2,t+1)} = 0.5\,[\,(1-\beta_{qi})\,x_j^{(1,t)} + (1+\beta_{qi})\,x_j^{(2,t)}\,]. \tag{14}$$

where x_i is the i^{th} child with $_qth$ component, x_j is the selected parent and β_{qi} (≥ 0) is a sample from a random number generated.

(b) Polynomial Mutation:

The probability of creating a solution near to the parent is higher than the probability of creating one distant from it. The shape of the probability distribution is directly controlled by an external parameter η_m and the distribution remains unchanged throughout the iterations. Like in the SBX operator, the probability distribution can also be a polynomial function, instead of a normal distribution:

The polynomial mutation is performed by

$$y_i^{(1,t+1)} = (x_j^{(1,t+1)} + (x_j^{(U)} - x_i^{(L)})\,\delta_i \tag{15}$$

where $y_i^{(1,t+1)}$ is the child and $x_j^{(1,t+1)}$ is the parent with $x_j^{(U)}$ being the upper bound on the parent component, $x_i^{(L)}$ is the lower bound and δ_i is small variation which is calculated from a polynomial distribution.

$$P(\delta_i) = 0.5(\eta_m + 1)(1-\delta i)^{\eta_m}, \tag{16}$$

$$\delta_i = \begin{cases} (2r_i)^{\frac{1}{(\eta_m+1)}} - 1, & \text{if } r_i \leq 0.5; \\ 1 - [2(1-r_i)]^{\frac{1}{(\eta_m+1)}}, & \text{if } r_i \geq 0.5; \end{cases} \tag{17}$$

r_i is an uniformly sampled random number between (0; 1) and η_m is mutation distribution index.

For handling the bounded decision variables, the mutation operator is modified for two regions, i.e. $[(x_j^{(L)} - x_i)]$ and $[(x_j - x_i^{(U)})]$.

6. *Recombination and Selection.* The offspring population is combined with the current generation population and selection is performed to set the individuals of the next generation. Since all the previous and current best individuals are added in the population, elitism is ensured. Population is now sorted based on non-domination. The new generation is filled by each front subsequently until the population size exceeds the current population size. If by adding all the individuals in front F_j the population exceeds N then individuals in front F_j are

selected based on their crowding distance in the descending order until the population size is N. And hence the process repeats to generate the subsequent generations.

The control parameters of NSGA-II must be adjusted to give the best performance. The parameters are: Probability of cross over P_c=0.9 with distribution index η_c=20, mutation probability P_m=0.25 and population size P_z=100. It was found that the NSGA-II with those control parameters produces better convergence and distribution of optimal solutions located along the Pareto optimal solutions. The 1000 generations are quite enough to find the true optimal solutions.

5. Results and discussion

The machining characteristics of Al/SiC_p composites are an important area of study. These materials are known as the difficult-to-machine materials because of the hardness and abrasive nature of reinforcement element-like silicon carbide particles (SiCp). Due to the above facts, achieving multiple performances is very difficult. The NSGAII is used for optimization to achieve better multiple performances.

The second-order polynomial model was developed for tool flank wear. The fit summary indicates that the quadratic model is statistically significant for analysis of flank wear. The value of R^2 is over 99.65%, which indicates that the developed regression model is adequately significant at a 95% confidence level. It provides an excellent relationship between the machining parameters and the responses tool flank wear.

An analysis of variance (ANOVA) was performed for tool flank wear and the results are presented in Table 3. The normal probability plot for tool flank wear is presented in Figure 2. It can be noticed that the residuals fall on a straight line, which means that the errors are normally distributed and the regression model is well fitted with the observed values. Figure 3 shows the residual values with fitted values for surface roughness. Figure 3 indicates that the maximum variation of -0.0100 to 0.0050, which shows the high correlation that exists between fitted values and observed values.

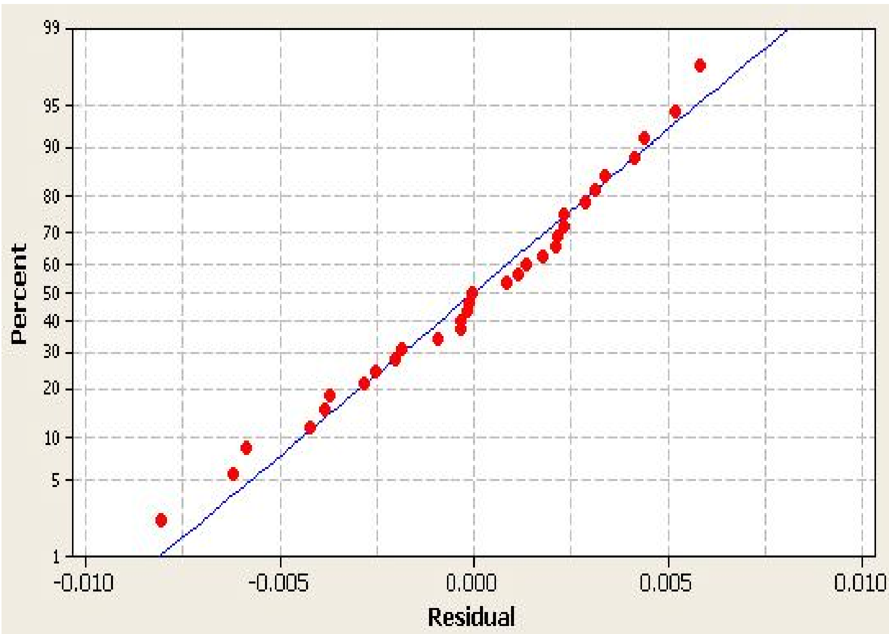

Figure 2. Normal probability plot for VBmax, mm

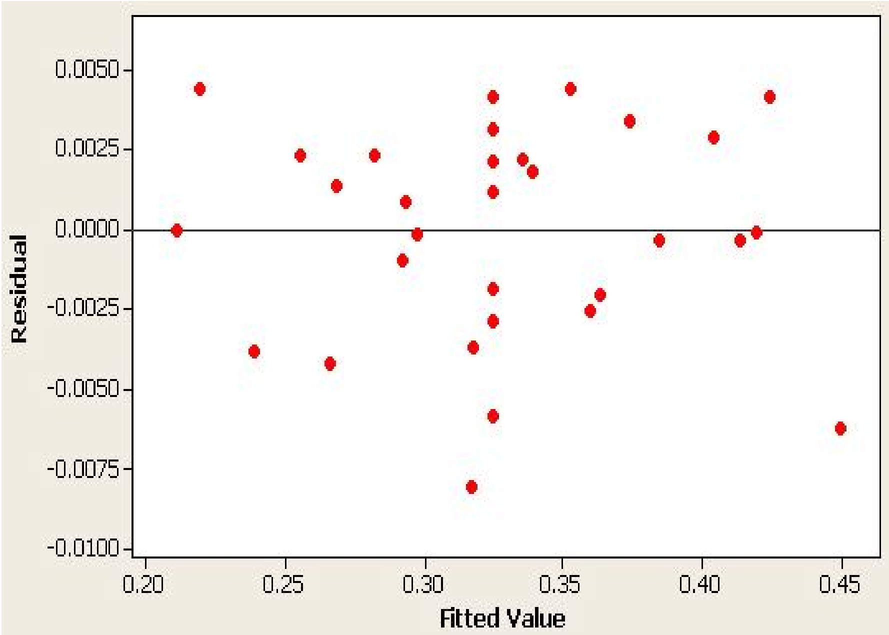

Figure 3. Residual versus fitted values for VBmax, mm

Table 3. Analysis of variance for flank wear, VB_{max}

Source of variation	Degree of freedom	Sum of squares	Mean sum of squares	*F*- value	p- value
Regression	14	0.103963	0.007426	328.73	0.000
Linear	4	0.102512	0.000268	11.88	0.000
Square	4	0.000642	0.000160	7.10	0.002
Interaction	6	0.000809	0.000135	5.97	0.002
Residual Error	16	0.000361	0.000023		
Total	14	0.103963			

Similarly, the value of R^2 for surface roughness is 99.85%, which means that the regression model provides an excellent explanation of the relationship between the independent variables (factors) and the response surface roughness. The associated p-value for the model is lower than 0.05 (i.e. level of significance α=0.05, or 95% confidence), which indicates that the model can be considered statistically significant. The result proves that the feed rate and spindle speed enhance the surface finish. The ANOVA table for the quadratic model for Ra is presented in Table 4. The model results indicate that the model is significant at a 95% confidence level. The normal probability of residuals for Ra is presented in Figure 4. It is observed that the residuals are distributed normally and in a straight line and hence the model is adequate. The fitted values versus the residuals are presented in Figure 5. The residuals observed are from -0.075 to 0.050, which shows the high correlation that exists between the model and experimental values.

In the present work, a non-dominated sorting genetic algorithm, NSGA-II, was used to optimize multiple performances using the second-order models created. The NSGA-II algorithm ranked the individuals based on dominance. The control parameters in NSGA-II were adjusted to obtain the best performance. The parameters used are: probability of crossover=0.9 with distribution index 20, mutation probability 0.25 and population size 100. It was found that the above control parameter produces better convergence and distribution of optimal solutions. The 100 generations were generated to obtain the true optimal solution. The non dominated solution set obtained over the entire optimization is shown in Figure 5. This figure shows the formation of the Pareto front leading to the final set of solutions. The 40 out of 100 sets were presented in Table 6; since none of the solutions in the non-dominated set is absolutely better than any other, any one of them is the "better solution". As the best solution can be selected based on individual product requirements, the process engineer must therefore select the optimal solution from the set of available solutions. If the engineer desires to have a better surface finish, or less flank wear on the tool, a suitable combination of variables can be selected from Table 5.

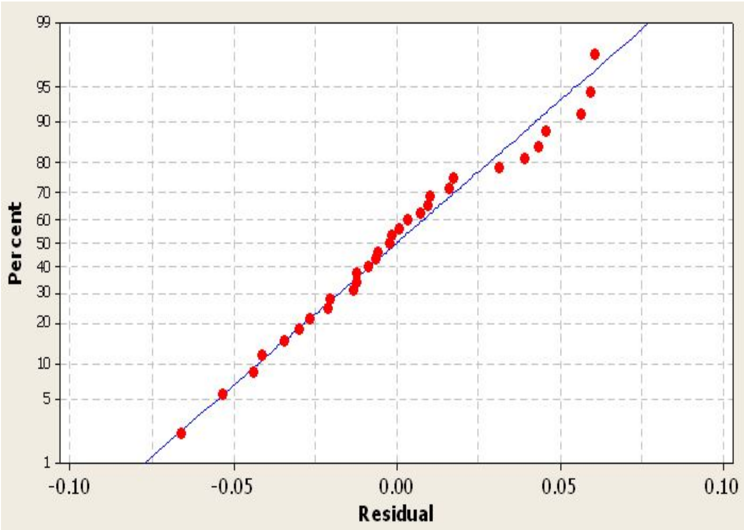

Figure 4. Normal probability plot for surface roughness, μm

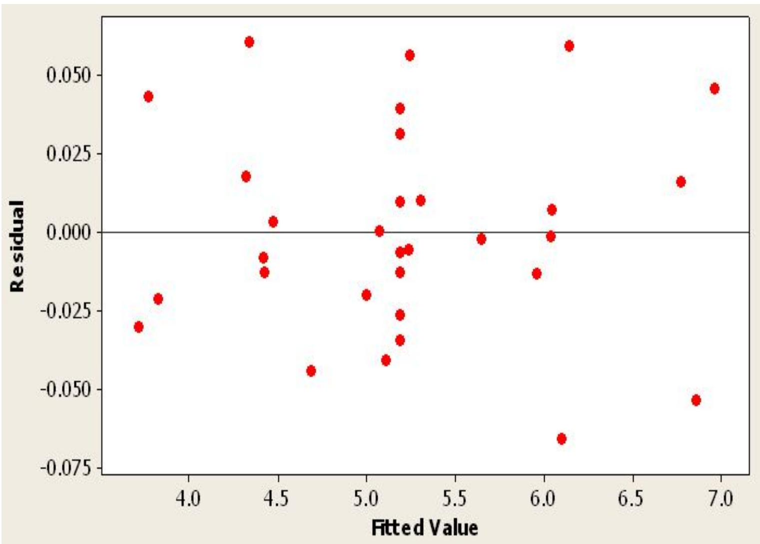

Figure 5. Residual versus fitted values for surface roughness, μm

Table 4. Analysis of variance for surface roughness, R_a

Source of variation	Degree of freedom	Sum of squares	Mean sum of squares	F- value	p- value
Regression	14	22.0127	1.572334	763.09	0.000
Linear	4	21.7361	0.078294	38.00	0.000
Square	4	0.2282	0.057041	27.68	0.000
Interaction	6	0.0485	0.008076	3.92	0.013
Residual Error	16	0.0330	0.002060		
Total	30	22.0456			

Table 5. Optimal combinations of parameters for end milling process

Ex.no	N, RPM	f, mm/rev	d, mm	S, %wt.	VBmax, mm	Ra, µm
1	2508.11	0.023	2.08	9.3	0.239	3.929
2	2744.99	0.021	1.09	12.08	0.252	3.783
3	2122.19	0.027	2.2	8.03	0.196	4.395
4	2271.40	0.020	0.81	12.0	0.216	4.171
5	3182.14	0.020	1.59	13.17	0.318	3.065
6	3685.33	0.020	0.66	5	0.364	2.570
7	2227.17	0.02	1.62	11.99	0.221	4.121
8	2530.47	0.02	1.04	9.07	0.253	3.775
9	3533.68	0.021	0.87	19.46	0.403	2.145
10	3638.67	0.020	0.52	5.11	0.414	2.027
11	3731.99	0.020	0.57	6.1	0.429	1.869
12	3806.48	0.020	0.5	5	0.434	1.752
13	3510.35	0.031	0.56	5.1	0.395	2.234
14	3055.40	0.021	1.38	16.4	0.332	2.921
15	2332.16	0.023	1.60	10.0	0.223	4.093
16	2658.79	0.022	1.91	7.2	0.274	3.549
17	2430.84	0.020	1.0	12.6	0.241	3.904
18	2239.04	0.03	0.69	5.3	0.213	4.204
19	2390.49	0.021	1.41	11.4	0.230	4.024
20	2145.52	0.030	1.15	5.34	0.200	4.349
21	3113.13	0.020	1.36	15.84	0.339	2.840
22	3137.02	0.02	1.9	16.19	0.342	2.809
23	3078.74	0.04	0.65	5.34	0.206	4.286
24	3997.01	0.02	0.9	5.02	0.466	1.461
25	2727.13	0.02	1.2	7.14	0.284	3.442
26	3198.75	0.02	1.41	10.1	0.351	2.706
27	3018.21	0.020	1.55	14.26	0.296	3.310
28	2171.94	0.02	1.5	6.4	0.204	4.308
29	3452.21	0.02	0.82	5	0.388	2.311
30	2078.25	0.02	0.57	8.2	0.191	4.454
31	4000.00	0.02	0.5	5	0.467	1.456

From the experimental results presented in Table 2, the parameters listed in the experiment number 19 lead to minimum *R*a of 3.679µm and the corresponding tool flank wear of 0.314mm, where the spindle speed, feed rate, depth of cut and %wt. of silicon carbide are 3000 RPM, 0.02mm/rev, 1.5mm and 15%, respectively. By using NSGA-II, the optimized *R*a value very close to the experimental value has been selected from Table 5. For trail No. 27, the surface roughness value is 3.310 µm and the corresponding tool flank wear is 0.296 mm, and the pertinent parameters are spindle speed, feed rate, depth of cut and %wt. of silicon carbide, which are 3018.21 RPM, 0.02mm/rev, 1.55mm, 14.26%, respectively. This indicates that the values obtained from the optimization technique are in close agreement with the experimental values and more or less for the same parameter settings.

The verification of the test results under the selected optimum conditions for the cases of tool flank wear and surface roughness are shown in Figure 6. The predicted machining performance is compared with the actual machining performance and a good agreement is obtained between their performances. From the analysis of Table 6, it can be observed that the calculated error is small. The error between the experimental and the predicted values for tool flank wear and surface roughness lie within 3% and 6%, respectively. Obviously, this confirms excellent reproducibility of the experimental conclusions.

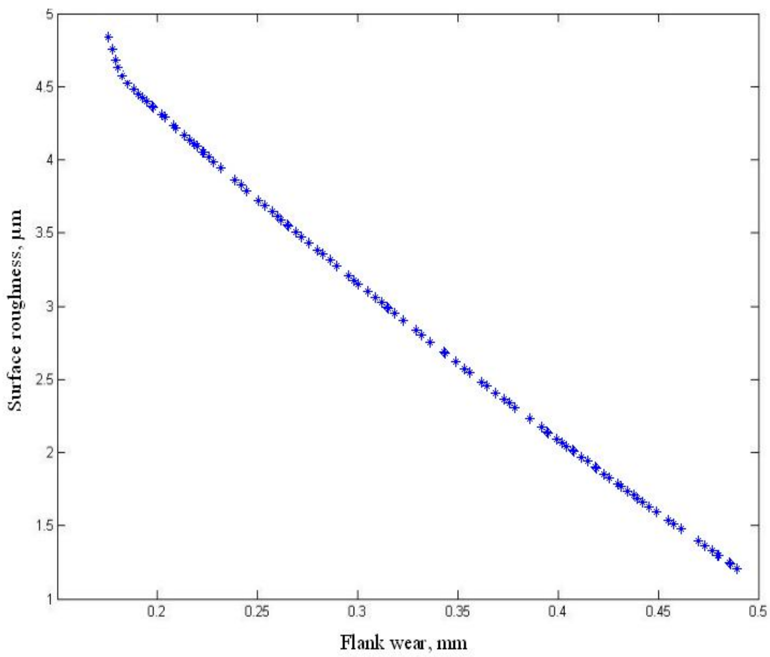

Figure 6. Pareto optimal chart obtained through NSGA-II

Table 6. Validation test results

Spindle speed (RPM)	Feed rate (mm/rev)	Depth of cut (mm)	Silicon Carbide (%wt.)	VB_{max}, mm			Surface roughness, µm		
				Predicted	Actual	Error %	Predicted	Actual	Error %
3018.21	0.020	1.55	14.26	0.296	0.304	3	3.310	3.507	6

6. Conclusion

a) The end milling process parameters were optimized by using non-dominated sorting genetic algorithm (NSGA-II), and a non-dominated solution set was obtained. The second order polynomial models developed for tool flank wear and surface roughness were used for optimization.
b) The choice of one solution over the other depends on the process engineer's requirements. If the requirement is a better Ra or lower VBmax, a suitable combination of variables can be selected.
c) The optimized value of Ra obtained through NSGA-II is 3.310μm and the corresponding VBmax is 0.296 mm, and the pertinent parameters are spindle speed, feed rate, depth of cut and wt. of silicon carbide, which are 3018.21 RPM, 0.02mm/rev, 1.55mm, 14.26%, respectively.
d) Optimization will help to increase production rate considerably by reducing machining time. The objectives such as tool flank wear and surface roughness were optimized using non-dominating sorting genetic algorithm-II. A Pareto-optimal set of 100 solutions was obtained.

References

[1] Manna, A. and Bhattacharyya, B. 2003. A study on machinability of Al/SiC-MMC. *Journal of Material Processing Technology*, 140: 711-716.
[2] Kevin Chou, Y. R. and Jie Liu. 2005. CVD diamond tool performance in metal matrix composite machining. *Journal of Surface and Coatings Technology*, 200: 1872-1878.
[3] Suresh Kumar Reddy, N., Shin, K. S., and Minyang, Y. 2008. Experimental study of surface integrity during end milling of Al/SiC particulate metal-matrix composites. *Journal of Material Processing Technol*, 201: 574-579.
[4] Li, X. and Seah, W. K. H. 2001. Tool wear acceleration in relation to workpiece reinforcement percentage in cutting of metal matrix composites. *Journal of Wear 2472*, 161-171.
[5] Ozben, T., Kilickap, E., and Cakir, O. 2008. Investigation of mechanical and machinability properties of SiC particle reinforced Al-MMC. *Journal of Mater Process Technol*, 198: 220-225.
[6] Kaye, J. E., Yan, D. H., Popplewell, N., and Balakrishnan, S. 1995. Predicting tool flank wear using spindle speed change. *Journal ofMach. Tools Manufact*, 35: 1309-1320.
[7] Srinivas, N. and Kalyanmoy, D. 1994. Multiobjective optimization using non-dominated sorting in genetic algorithms. *Journal of Evol. Comp*, 2(3): 221-248.
[8] Kanagarajan, D., Karthikeyan, R., Palanikumar, K., and Davim, J. P. 2008. Optimization of electrical discharge machining characteristics of WC/Co composites using Non-dominated sorting genetic algorithms (NSGA-II) . *Journal of Advd Mfg Technol*, 36: 1124-1132.
[9] Kuriakose, S. and Shunmugam, M. S. 2005. Multi-objective optimization of wire electro discharge machining process by non-dominated sorting genetic algorithm. *Journal of Materials Processing Technology*, 170: 133-141.
[10] Raghuwanshi, M. M. and Kakde, O. G. 2004. Survey on multi-objective evolutionary and real coded genetic algorithm. In: Proceedings of the 8th Asia-Pacific Symposium on Intelligent and Evolutionary Systems, Cairns, Australia. 150-161.
[11] Akundi, S. V. K., Simpson, T. W., and Reed, P. M. 2005. *Proceedings of ASME Computers*

and Information in Engineering Conference, Paper No: DETC 2005/DAC-84905, California, USA.
[12] Boothroyd, G. 1983. "*Fundamentals of Metal Machining and Machine Tools*". McGraw-Hill Book Co., London.
[13] Juneja, B. L. and Sekhon, G. S. 2000. "*Fundamentals of Metal Cutting and Machine Tools*". New Age International (P) Limited Publishers, India.
[14] Subramanian, R., Subramanian, K., and Subramanian, B. 2009. Application of a fast and elitist multi-objective genetic algorithm to reactive power dispatch. *Serbian Journal of Electl. Engg*, 6(1): 119-133.